Aurora Iris Agate

When solar wind interacts with the earth's magnetosphere, spectacular multicolor light shows occur. This phenomenon is referred to as an aurora borealis in the Northern Hemisphere and an aurora australis in the Southern Hemisphere. This author recently examined an iris agate that provided a microscopic scene remarkably similar to an aurora (figure 1). The 1.67 ct carving seen in figure 2 was fashioned by Falk Burger (Hard Works, Tucson, Arizona). Burger took advantage of this quartz's unique growth texture by carving the agate's back, producing a wispy iridescent effect that is visible when using a point light source. Along the lower portion of the gem was a thin layer of crystalline quartz with a seam of pyrolusite dendrites between the crystalline quartz and microcrystalline iris agate. The combination of these layers gives the viewer the impression of an aurora occurring over a forest-rimmed frozen lake (see video at www.gia.edu/gems-gemology/aurora-iris-agate-carving).

Nathan Renfro
GIA, Carlsbad

Figure 1. In transmitted light, this skillfully carved iris agate displays a scene reminiscent of an aurora. Photomicrograph by Nathan Renfro; field of view 5.28 mm.

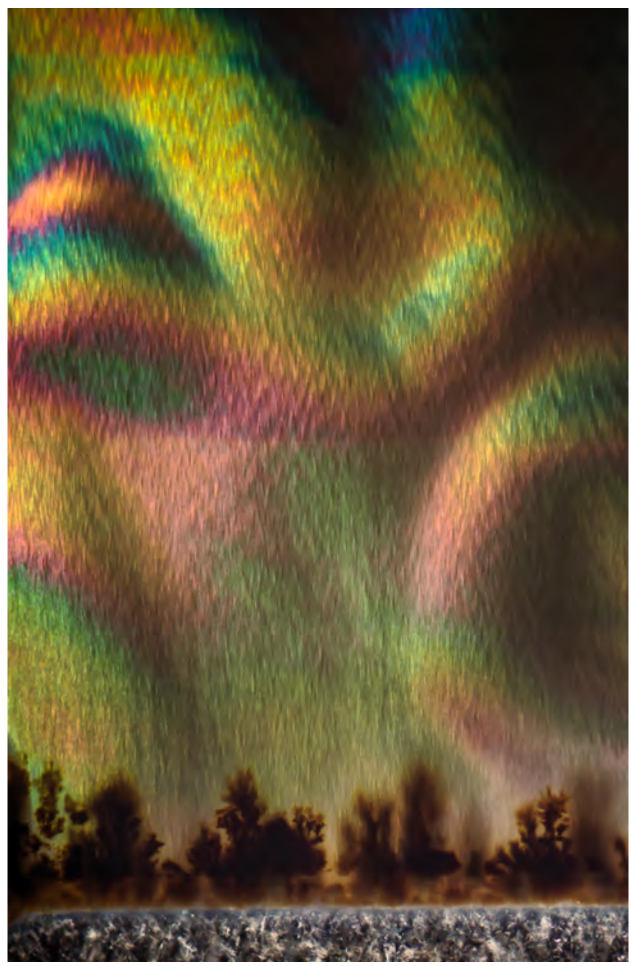

Inclusions in Burmese Amber

Burmese amber has been well documented in the paleontological literature, but is overshadowed in the gemological

About the banner: Columnar hexagonal graining, seen in some Colombian emeralds, creates a roiled appearance called gota de aceite *(Spanish for "drop of oil"). The optical effect is seen here using shadowed transmitted illumination. Photomicrograph by Nathan Renfro; field of view 3.23 mm.*

Editors' note: Interested contributors should contact Nathan Renfro at nrenfro@gia.edu and Jennifer-Lynn Archuleta at jennifer.archuleta@gia.edu for submission information.

GEMS & GEMOLOGY, VOL. 52, NO. 2, pp. 198–205.

Figure 2. The 1.67 ct iris agate, shown here in transmitted light (left) and reflected light (right) was carved to showcase the dynamic nature of the iridescent colors. Photos by Kevin Schumacher.

community by material from the Dominican Republic and the Baltic area. Despite the armed conflict in the Hukawng Valley, possibly the world's largest tiger reserve, accessibility has improved and amber production has steadily increased since 2014. As a result, more Burmese amber is reaching the marketplace. We have observed rising interest in the Bangkok, China, and Hong Kong markets, with specimens containing large inclusions of flora and fauna in great demand and commanding high prices. The samples presented here (figures 3–5) were acquired during a January 2016 field expedition to the Hukawng Valley and are now part of the GIA research collection.

These amber specimens are interesting because they potentially preserve evidence from biological environments of 80 to 100 million years ago (G. Shi et al., "Age constraint on Burmese amber based on U–Pb dating of zircons," *Cretaceous Research*, Vol. 37, 2012, pp. 155–163, www.sciencedirect.com/science/article/pii/S0195667112000535). They are significantly older than amber from the Dominican Republic, estimated at 25–40 million years old) and the Baltic region, which are about 25–28 million years old (D. Penney, *Biodiversity of Fossils in Amber from the Major World Deposits*, Siri Scientific Press, Manchester, United Kingdom, 2010).

Victoria Raynaud, Vincent Pardieu, and Wim Vertriest
GIA, Bangkok

Figure 3. This Tropidogyne *flower is still attached to its stem and has a small flea-like bug near its right side, as seen with darkfield and fiber-optic illumination. Photomicrograph by Victoria Raynaud; field of view 5.97 mm.*

Figure 4. This spider is surrounded by small air bubbles and plant debris. It is very easy to resolve fine details, such as individual hairs and different sets of eyes. The sample is illuminated with a combination of diffuse brightfield and fiber-optic light. Photomicrograph by Victoria Raynaud; field of view 7.20 mm.

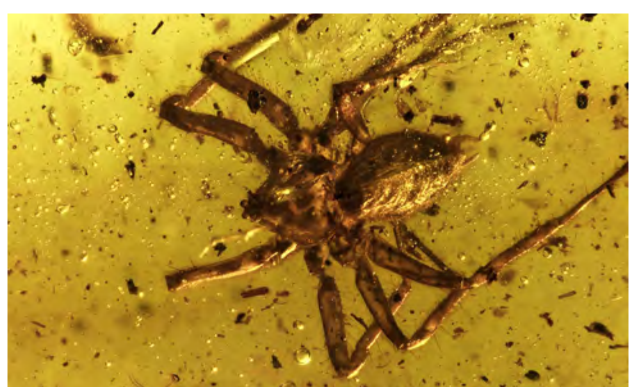

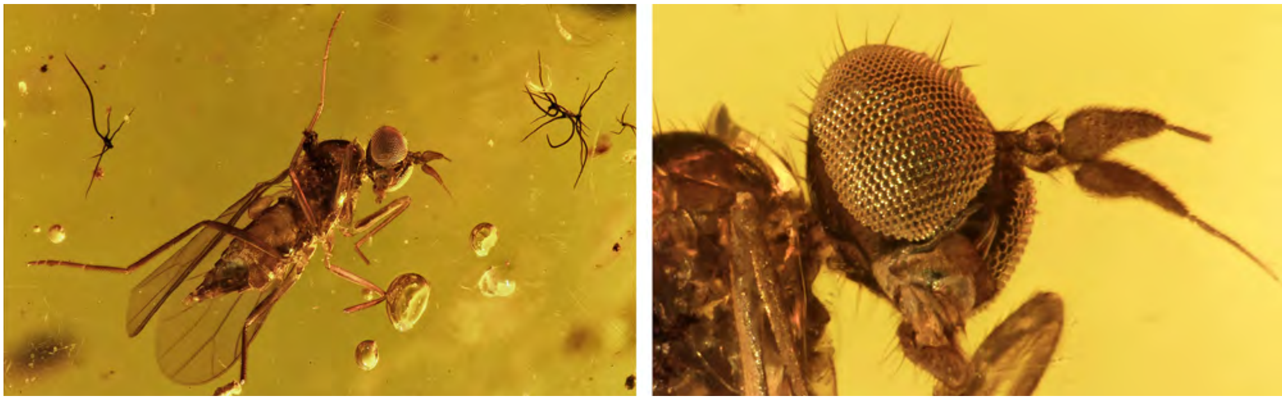

Figure 5. Left: The delicate features of this fly, particularly its wings, are surrounded by gas bubbles and trichomes (hair-like structures that grow on plants). Right: This image demonstrates the excellent preservation qualities of amber, as evidenced by the detailed structure of the fly's eye. Photomicrographs by Victoria Raynaud; field of view 4.80 mm (left) and 0.86 mm (right). Brightfield and fiber-optic illumination.

Chalcedony with Quartz Windows

A translucent white chalcedony specimen containing a few small transparent quartz crystals was fashioned into a decorative polished plate by Falk Burger (Hard Works, Tucson, Arizona). One intriguing feature of this piece is that most of the transparent quartz crystals were aligned with their c-axes parallel to each other. When they were transected perpendicular to this axis during the polishing process, angular transparent windows were created, each displaying trigonal symmetry within their otherwise translucent chalcedony host. Interestingly, even though the white chalcedony was polished into a plate, it still showed a rather curious angular-looking three-dimensional texture. When examined between crossed polars,

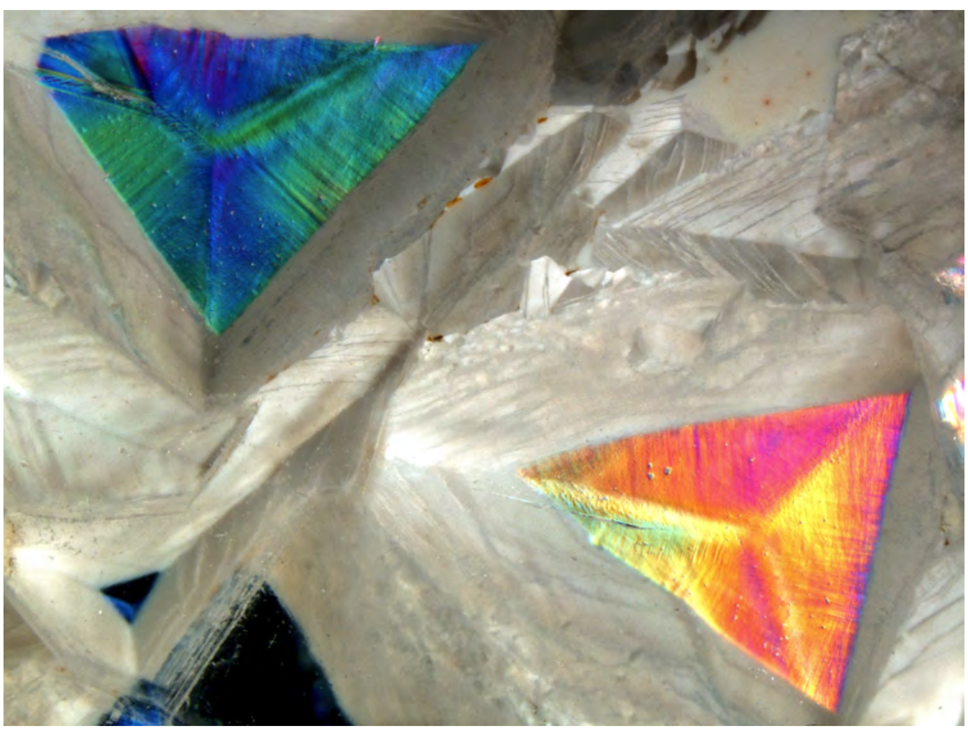

Figure 6. The trigonal windows of quartz found throughout this translucent white chalcedony displayed vibrant interference colors when examined between crossed polars. The black triangles in the lower left corner are also quartz. Photomicrograph by John I. Koivula; field of view 15.5 mm.

Figure 7. "Pond Life," a 50.95 ct orbicular chalcedony cabochon measuring 48.5 × 27.0 × 5.5 mm, evokes a pond. The "frog eggs" are actually iron-containing inclusions surrounded by the host's concentric growth. Photo by Elise A. Skalwold.

the triangular quartz windows ignited with vibrant interference colors (figure 6) due to Brazil-law twinning in the crystals.

John I. Koivula
GIA, Carlsbad

"Pond Life" Orbicular Chalcedony

The seemingly infinite combination of growth features and inclusions seen in microcrystalline quartz fires the imagination, often evoking visual metaphors (see "Aurora Iris Agate" in this column). Such is the case with the orbicular chalcedony seen in figure 7. From a piece of non-descript tumbling rough purchased in 2011, Paul Stalker (Stones by Stalkers, Tioga, Pennsylvania) delighted in creating what he christened "Pond Life," as the 50.95 ct piece's polished appearance resembles frog eggs within a pond.

Exploring the interior of such microcrystalline varieties of jaspers and agates can be just as fascinating as exploring inclusions within single-crystal quartzes, though these opportunities may be overlooked when dazzled by complex macro features. Orbicular chalcedonies such as this ocean jasper are particularly interesting. Here, iron-containing inclusions such as limonite, goethite, and hematite are surrounded by the concentric growth of the host material, which displays the unique fibrous texture found in some types of chalcedony (figure 8, left). Bundles of fibers composed of crystallites are combined with mutually complex optical orientations, giving rise to the eye-visible effect. While beautiful in transmitted, reflected, and polarized light, the addition of various contrast filters can dramatically enhance the details of these subtle growth features, making them easier to study, as well as creating stunning images of a specimen's inner world (figure 8, right). For more on advanced filtering techniques, see Fall 2015 Micro-World, pp. 328–329.

Elise A. Skalwold
Ithaca, New York

Garnet Inclusion Illusion

A cleverly designed "garnet in quartz" double cabochon represents a new and unexpected challenge for gemologists, collectors, and designers who intend to feature inclusion gemstones in their jewelry lines. This assembled inclusion consists of a fragment of pyralspite-series garnet sandwiched between two quartz cabochons (figure 9). The garnet and quartz were identified with optical and Raman spectroscopy, respectively, at GIA's Carlsbad laboratory. While the specimen creates the illusion of being natural, clues to its artificial origin include air bubbles and the fragment itself, which shows neither crystal faces nor the rounded appearance of an etched or eroded crystal. Rather,

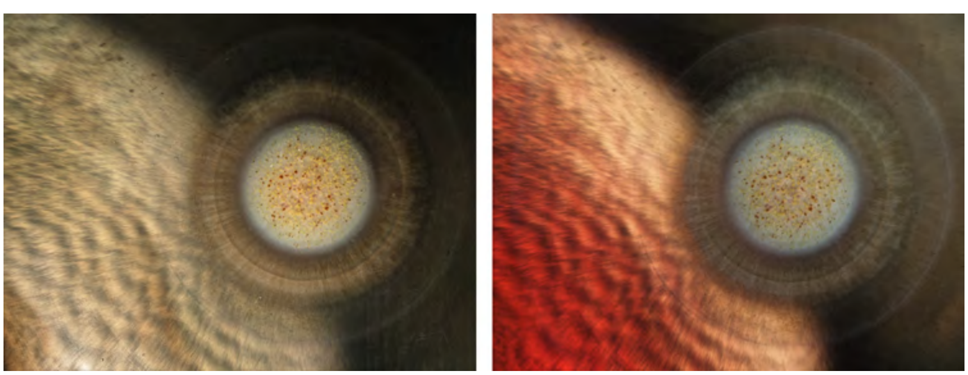

Figure 8. The use of a red contrast filter with transmitted light (left) dramatizes growth textures, making them easier to study than with unfiltered transmitted light (right) while creating an aesthetically pleasing image. Photomicrograph by John I. Koivula; field of view 4.0 mm.

Figure 9. At first glance, this 42.88 ct quartz double cabochon measuring 28 × 18.5 × 15 mm resembles a beautiful garnet-included quartz gem. Photo by Elise A. Skalwold, from the Si and Ann Frazier Collection.

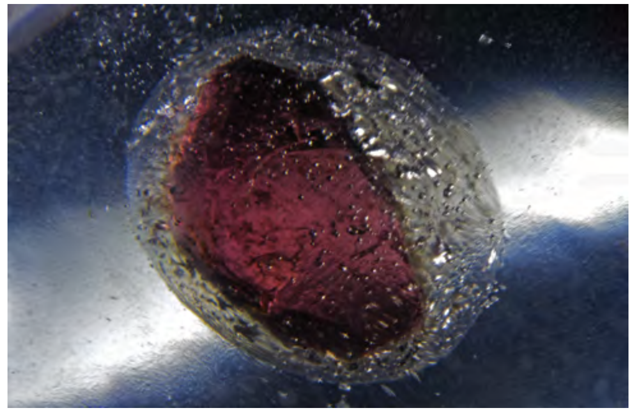

Figure 10. Gas bubbles can be seen in an otherwise nearly invisible glue layer between the quartz cabochons; these bubbles are abundant in the vicinity of the red garnet fragment. The fragment resides in a hollowed-out pocket and is surrounded with glue. Photomicrograph by Nathan Renfro; field of view 10.28 mm.

it is a relatively sharp fragment that resides in a pocket filled with glue (figure 10). The subtle glue layer between the cabochons becomes more apparent when viewed under UV light, which causes it to fluoresce chalky white; this fluorescence is stronger under long-wave than short-wave UV.

This specimen was purchased at the 2016 Tucson shows from a dealer specializing in inclusion specimens. The cabochon, part a collection of otherwise natural items, was fully disclosed as a man-made novelty. Its appearance in the marketplace represents an emerging trend that gemologists and collectors will see with increasing regularity as the fascination with inclusions grows (see the author's forthcoming article, "Evolution of the inclusion illusion," in the Summer 2016 *InColor*). Careful inspection with a loupe or microscope will in most cases reveal the underlying nature of this inclusion.

Elise A. Skalwold

Iridescent *Spondylus* Pearl

The optical phenomenon of iridescence is frequently observed in gem materials, but it is uncommon to see iridescent colors in porcelaneous pearls. Such pearls are appreciated for their prominent eye-visible flame structures, such as those seen in some Queen conch and Melo pearls. Pearls from these gastropods, along with *Spondylus* species bivalves, are routinely submitted to GIA's laboratory. A bluish reflective sheen is a common feature of the flames seen in *Spondylus* pearls (Fall 2014 Lab Notes, pp. 241–242; Winter 2015 Lab Notes, pp. 436–437).

A 6.97 ct bicolored white and pink *Spondylus* pearl (figure 11) was recently examined at GIA's Carlsbad labora-

Figure 11. This 6.97 ct bicolored white and pink Spondylus *pearl shows prominent reflective blue coloration over the fine parallel flame structure when viewed in certain directions under a single white light source. Photo by Robert Weldon/GIA.*

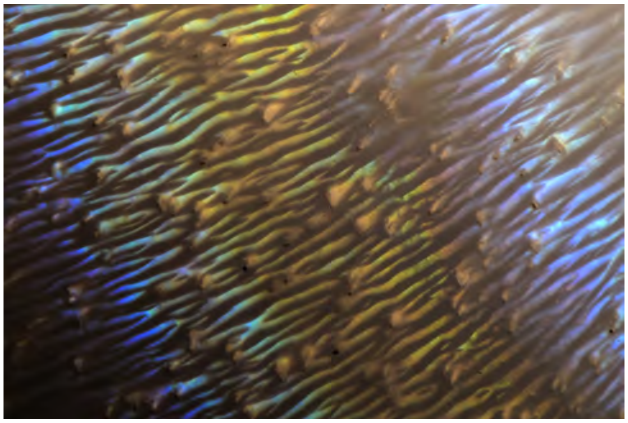

Figure 12. Under magnification and using fiber-optic illumination, iridescent colors ranging from purplish to dominant blue reflect from the fine, well-formed flame structure of this Spondylus *pearl. Photomicrograph by Artitaya Homkrajae; field of view 2.34 mm.*

Figure 13. The prominent sulfide inclusion in this 2.02 ct pyrope is clearly visible under the table facet. Photo by Kevin Schumacher.

tory. When a single white light was used to illuminate the pearl, a prominent reflective blue coloration over its fine parallel flame structure was visible on the white portions. This created a pseudo-chatoyant effect similar to other *Spondylus* pearls previously examined. What was particularly captivating about this pearl was that iridescent colors ranging from purplish to a dominant blue were seen on the fine, well-formed flame structure when a fiber-optic light was applied in certain directions (figure 12).

As with many gemstones and nacreous pearls, the spectral colors seen on the flame structure are the result of the interference effect of light reflecting off of structural features. In this case, the thickness of the aragonite lamellae permits white light to be diffracted into most of the visible light wavelengths, resulting in a colorful effect.

The iridescence characteristics of this pearl have not been encountered to such a marked degree in any other porcelaneous pearl examined by GIA.

Artitaya Homkrajae
GIA, Carlsbad

Metal Sulfide in Pyrope

The 2.02 ct "inclusion gem" shown in figure 13 is not only spectacular to inclusion enthusiasts, but also a scientific mystery. This vanadium- and chromium-bearing pyrope was cut from one of the samples featured in *G&G*'s Winter 2015 issue (Z. Sun et al., "Vanadium- and chromium-bearing pink pyrope garnet: Characterization and quantitative colorimetric analysis," pp. 348–369). The stone was faceted by Jason Doubrava (Poway, California) to display a relatively large, euhedral sulfide crystal inclusion. Sulfide crystals were observed in several of the samples in the 2015 study; the exact nature of the inclusions could not be determined by Raman analysis, but all displayed a metallic luster in surface-reflected light. Magnification also revealed a cloud of minute acicular inclusions resembling rutile surrounding the crystal (figure 14). Along with the elements expected for pyrope, such as Si, Al, Mg, Mn, and Fe, energy-dispersive X-ray fluorescence (EDXRF) analysis detected peaks for sulfur and rhodium. While sulfur would be expected in a metal sulfide, the rhodium peak is a mystery. Rhodium sulfide does exist, but explaining the presence of rhodium in this garnet would require destructive testing. In this case beauty trumps science, because this gem is truly a wonderful ad-

Figure 14. A cloud of extremely fine acicular inclusions in the pyrope surrounds the sulfide when viewed under the microscope with diffuse reflected light. Photomicrograph by Nathan Renfro; field of view 5.41 mm.

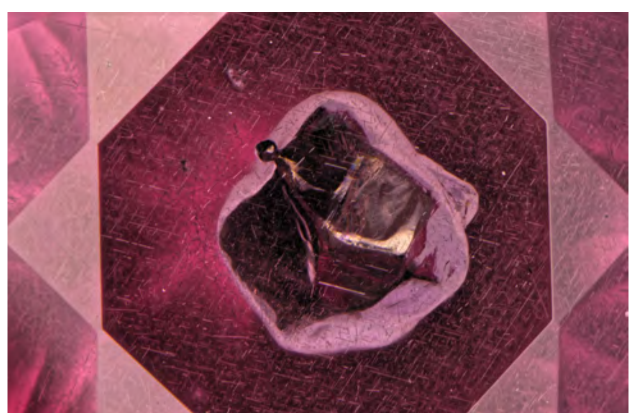

dition to the collection of this inclusionist and will thus remain a gemological curiosity.

John I. Koivula

Metallic Chromium Inclusions in Industrial By-Product Ruby

Technogenic corundum contained in metallurgical slag represents a potentially unique source of gem material. Since the 1950s, slags have been studied for their secondary uses. Their mineralogical and petrographic attributes have been documented, but to date there have been virtually no studies from a gemological standpoint.

X-ray powder diffraction analysis (XRD) was performed on two slag samples taken from the waste products of chromium ore processing by thermite reaction at a refinery located in Russia's Ural Mountains. These specimens showed the presence of corundum (α-Al_2O_3), the rare phase diaoyudaoite $NaAl_{11}O_{17}$, and a spinel-group mineral. For the spinel-group mineral, electron microprobe analysis (EPMA) indicated significant amounts of Mg, Cr, and Al. As seen in figure 15, the corundum contains transparent purplish red crystals up to 2.5 cm in length embedded in a diaoyudaoite matrix. The crystals may be elongated and prismatic, irregularly formed, or rounded. Gemological testing including refractometry, specific gravity measurements, and reaction under short-wave (254 nm) and long-wave (365 nm) UV. The UV reaction (figure 16, left) was consistent with natural and synthetic ruby (for in-depth analytical procedures and results, see E.S. Sorokina et. al., "On the question of technogenic ruby in the slags of Cr-V production," *Mine Surveying and Using of Mineral Resources,* Vol. 2, 2010, pp. 33–35, in Russian). Microscopic examination of the samples showed features such as gas bubbles and irregular growth lines, both of which are inconsistent with natural corundum. Most significant was the presence of a metallic-phase chromium that appeared in several forms, such as needles, dendrites, and rounded or irregularly formed black solid inclusions with metallic luster. The metallic chromium was most frequently observed along the ruby parting planes (figure 16, right); it is an inclusion that has never been detected in naturally occurring corundum or in any synthetic analogues.

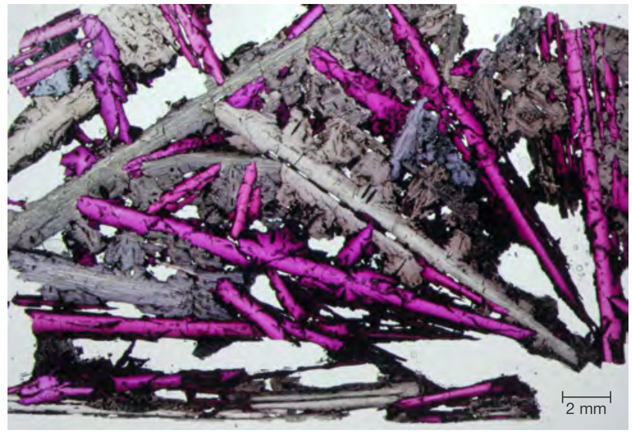

Figure 15. Photomicrograph of a petrographic thin section of ruby (purplish red)-diaoyudaoite (grayish green) slag, shown in transmitted light. From Sorokina et al. (2010).

Laser ablation–inductively coupled plasma–mass spectrometry (LA-ICP-MS) and EPMA showed high Cr content (4.3–7.7 wt.%), most likely linked to the capture of micron-sized metallic chromium inclusions during the measuring process. We also found 135–270 ppmw of Mg, 30–70 ppmw of Ti, and 5–10 ppmw of V. Fe, Ga, Ni, Pb, and

Figure 16. Left: Intense red photoluminescence typical of ruby observed under long-wave UV; field of view 8.34 mm. Right: Strongly reflecting rounded and irregularly shaped metallic chromium inclusions within the technogenic ruby, surrounded by greenish gray diaoyudaoite matrix. Shown in reflected light; field of view 0.288 mm. Photomicrographs by Elena S. Sorokina.

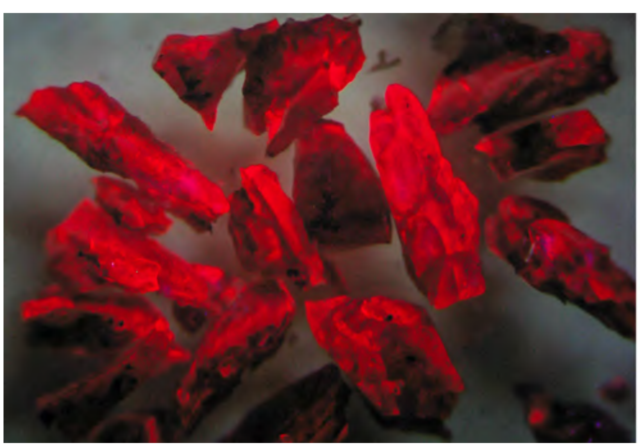

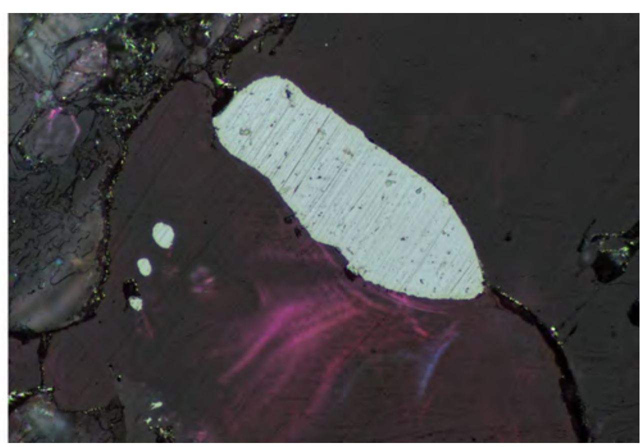

Figure 17. A pinkish orange inclusion dominates the interior of this 20.58 ct unpolished topaz crystal from Pakistan. Photograph by Kevin Schumacher.

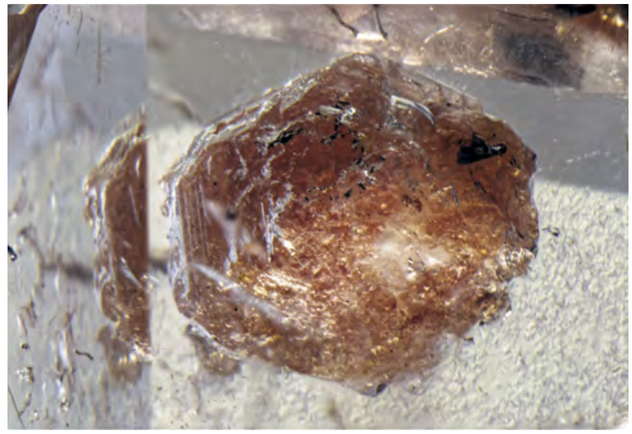

Figure 18. A combination of Raman and EDXRF analysis served to identify the inclusion as triplite. The inclusion is seen here using brightfield and fiber-optic illumination. Photomicrograph by Nathan Renfro; field of view 9.39 mm.

Pt were found to be below detection limit by both methods. This was the first time LA-ICP-MS had been applied to technogenic ruby.

The identification of metallic-phase chromium inclusions, coupled with trace-element chemistry, will serve to separate these ruby slag materials from natural and other artificial analogues.

Elena S. Sorokina
GIA, Carlsbad
Fersman Mineralogical Museum
Russian Academy of Sciences, Moscow

John I. Koivula
GIA, Carlsbad

Vladimir Karpenko
Fersman Mineralogical Museum
Russian Academy of Sciences, Moscow

Quarterly Crystal: Triplite in Topaz

The transparent colorless 20.58 ct topaz crystal in figure 17 clearly hosts a prominent translucent pinkish orange inclusion. The topaz, from Biensa in Braldu Valley, Gilgit-Baltistan, Pakistan, was acquired from Dudley Blauwet of Mountain Minerals International (Louisville, Colorado). The bodycolor of the inclusion suggested that it might be either of two equally rare pegmatitic phosphates, triplite or väyrynenite, that are known to occur in pegmatites in that part of the world (figure 18).

Laser Raman microspectrometry was able to narrow the inclusion's identity to these two suspected phosphates. Triplite and väyrynenite have very similar Raman peak patterns, and the topaz host masked some of the significant peaks needed to conclusively separate the two minerals. Since triplite contains iron and väyrynenite does not, focused energy-dispersive X-ray fluorescence (EDXRF) analysis was used to examine the inclusion's chemical composition. Results indicated the presence of iron, identifying the inclusion as triplite. This marks the first time triplite has been reported as an inclusion in topaz.

John I. Koivula

For More on Micro-World

To watch a video of the aurora like scene in the carved iris agate featured in this section, please visit http://www.gia.edu/gems gemology/aurora iris agate carving, or scan the QR code on the right.